Effect of Ultrasound on Thrombus debris during Sonothrombolysis in a Microfluidic device

Xiaobing Zheng[1] · Yunfan Pan[1] · Zhaojian Wang[2] · Shuguang Zhang[1]

Abstract

Microbubble-mediated sonothrombolysis has been proven to be a non-invasive and efficient method for thrombolysis. Nevertheless, there is a potential risk that the thrombus debris generated during the dissolution of the original thrombus are too large and can lead to hazardous emboli. Using a sonothrombolysis microfluidic platform, we investigated the effects of ultrasound power, thrombolytic agent and microbubble concentration on the size of thrombus debris with the example of microbubble-mediated sonothrombolysis of arterial thrombus. Additionally, we studied the effects of ultrasound power on the size and shape of thrombus debris produced by acute and chronic arterial sonothrombolysis. In acute arterial sonothrombolysis, ultrasound power has significant effect on the size of thrombus debris and steadily increases with the increase of ultrasound power. Conversely, in chronic arterial sonothrombolysis, the size of thrombus debris is minimally affected by ultrasound power. Using the sonothrombolysis microfluidic platform, the relationship between ultrasound power and the safety of sonothrombolysis has been illustrated, and the sonothrombolysis microfluidic platform is demonstrated to be a promising tool for further studies on the process of sonothrombolysis.

Graphical abstract
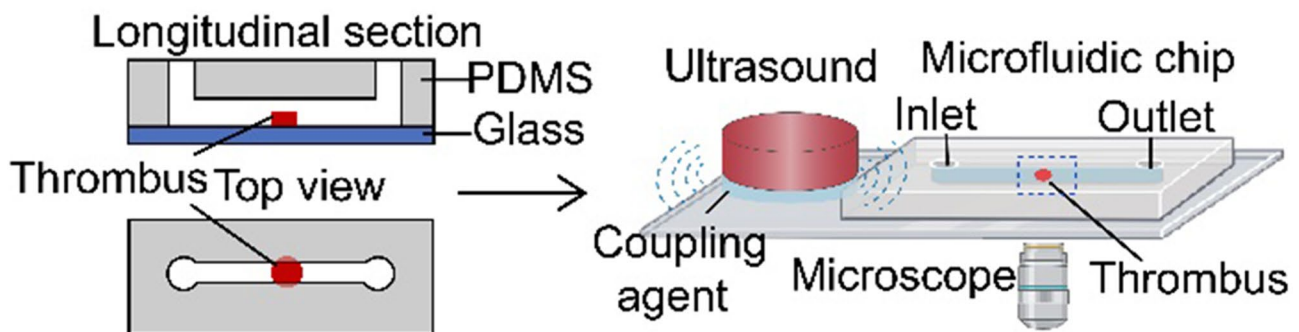
We explore the effect of microbubble-mediated sonothrombolysis parameters on the production of thrombus debris in a sonothrombolysis microfluidic platform, with the example of microbubble-mediated sonothrombolysis of arterial thrombus. (Left) Different views of the microchannel. (Right) The microfluidic system for sonothrombolysis.

Highlights

● The effect of ultrasound power on the size and morphological characteristics of thrombus debris was studied in a microfluidic device.
● The sonothrombolysis process of acute and chronic arterial thrombosis is emphasized.
● The mechanical action of ultrasound and the biochemical action of thrombolytic agents are matched in different ways, resulting in debris of different composition and size.
● This study may also help to implement safer thrombolysis strategies.

Extended author information available on the last page of the article

Introduction

Thrombosis, or blood clot developing in the vascular system, is a primary cause of vascular diseases [1]. Currently, the most common treatment for thrombosis is thrombolytic agent tissue plasminogen activator (tPA) therapy. However, its usage is limited as current guidelines indicate that it must be provided within 4.5 h of the symptom onset. Moreover, thrombolytic therapy is associated with a symptomatic hemorrhagic complication rate of around 7% [2, 3]. While ultrasound has been demonstrated to enhance thrombolysis [4]. The use of ultrasound is usually combined with the injection of thrombolytic agents [5] or ultrasound contrast agents (microbubbles) [6] to treat thrombosis, which is superior to standard endovascular thrombolytic agent therapy. Sonothrombolysis utilizes the mechanical effect of ultrasound to "loosen" the thrombus and increases the diffusion of the thrombolytic agent into the thrombus, resulting in faster and more effective thrombolytic therapy, which can reduce the dose of the thrombolytic agent and the treatment time of patients [7]. Although sonothrombolysis has been shown to be effective, the large-sized thrombus debris, which may form after thrombolysis, may obstruct downstream vessels [8]. Therefore, it is generally accepted in the medical community that thrombolytic techniques should be evaluated based on their ability to minimize thrombus debris.

Ultrasound-induced thrombus rupture is thought to be mainly caused by acoustic cavitation [9, 10], including stable cavitation and inertial cavitation [7]. Stable cavitation bubbles usually form microstreams in the vicinity of the thrombus, accelerating the diffusion of thrombolytic agents into the fibrin matrix. The violent oscillations and rapid collapse of inertial cavitation bubbles lead to localized pressure changes and high-speed microjets jetting onto the thrombus surface, mechanically tearing debris from the thrombus surface [11], as shown in Fig. 1A. The interaction between ultrasound and thrombus tissue is a hot topic in the study of sonothrombolysis. There are some studies addressing factors that affect the size of thrombus debris
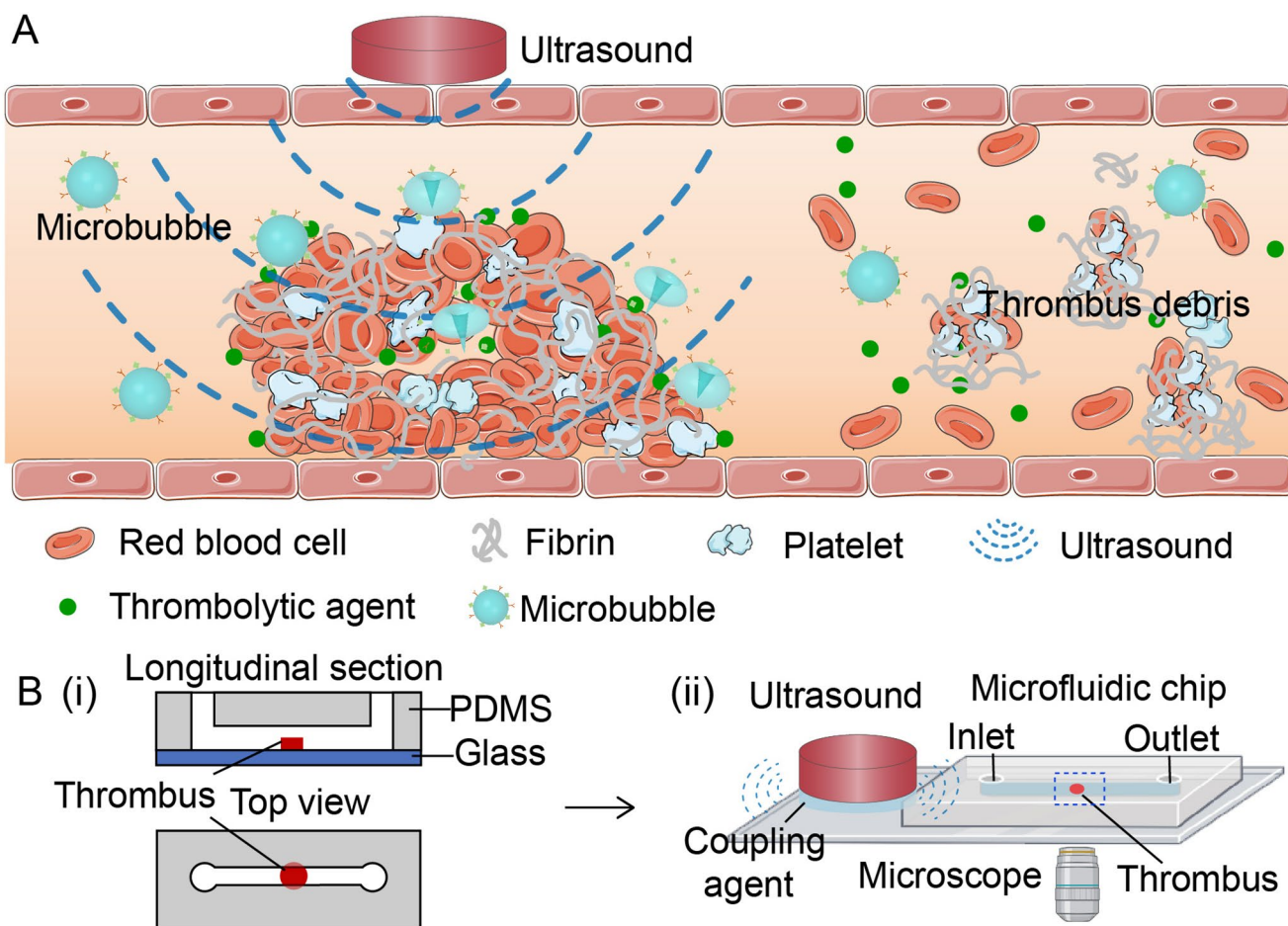
Fig. 1 The schematics illustrations of microbubble-mediated sonothrombolysis in thrombosis of artery. (A) In sonothrombolysis, the size of the thrombus debris produced by primary thrombus thrombolysis varies from large to small. (B) (i) Different views of the microchannel. (ii) The microfluidic system for sonothrombolysis

during sonothrombolysis. The effects of acoustic pressures, duty cycle and the size distribution of cavitation bubbles on the size of thrombus debris have been investigated [9, 12]. The effects of parameters involved in sonothrombolysis, such as ultrasound, microbubble and thrombolytic agents, on thrombus debris need to be further investigated. Large-sized thrombus debris, such as those ranging from 18 to 60 μm in diameter, have been shown to be occlusive and may lead to permanent cerebral ischemia [13]. Several studies on sonothrombolysis of different kinds of thrombus have demonstrated that thrombus density and structure, etc., can lead to different sensitivities to thrombolysis [14, 15]. However, there are limited studies addressing the characteristics of thrombus debris produced by thrombi of different ages.

In this paper, we aim to explore the effects of ultrasound power, thrombolytic agent and microbubble concentration on the size of thrombus debris generated during arterial thrombolysis using a sonothrombolysis microfluidic platform. Finally, the distribution and the composition of acute and chronic arterial thrombus debris under different ultrasound powers were further measured and analyzed.

Methods

Orthogonal Test Design

Orthogonal experimental design is an efficient and time-saving method to study multiple factors and levels. To analyze the effects of several parameters on the size of thrombus debris during sonothrombolysis, four levels of ultrasound power were selected from low to high: 0 W, 1.5 W, 3 W, and 6 W. Thrombolytic agents used in this work is tPA (Actilyse, Boehringer Ingelheim Pharma GmbH&Co, KG). In the in vitro studies, the safe dose of tPA used in humans varies from 0.1 to 100 μg/mL [16], and most studies use 3 μg/mL tPA, which corresponds to the blood concentration (0.9 mg/kg body weight) achieved with conventional intravenous dosing of tPA [17]. Four levels of thrombolytic agent concentrations were used: 0 μg/mL, 2.5 μg/mL, 12.5 μg/mL, and 25 μg/mL, representing the drug concentration under different treatment conditions. Microbubble concentrations were set as (0, 0.1, 1, and 10) $\times 10^7$ MBs/mL, representing conventional treatments and the maximum concentration of microbubbles used in clinical. The specific parameters of each experiment are listed in *Supplementary Materials B* (Table S1).

Microfluidic System of Sonothrombolysis

To observe the effect of ultrasound power on thrombus debris during sonothrombolysis in real time, we designed a microfluidic system for sonothrombolysis, as shown in Fig. 1B. The microfluidic chip is a 500 μm (W)×500 μm (H)×20 mm (L) channel with a glass slide at the bottom and the remaining three sides are made of polydimethylsiloxane (PDMS, Sylgard 184 kit, Dow Corning, density 1.05 g/cm³). A blood clot approximately 1 mm in length, greater than 500 μm in width and less than 500 μm in height was placed on the slide, and then a microfluidic chip which is a straight PDMS channel with 500 μm (W) × 500 μm (H) × 20 mm (L) was placed over the clot on the slide. Finally, the slide and microfluidic chip were clamped in place to prevent leakage, as shown in Fig. 1B(i). The clot did not completely occlude the channel and the flow is present. Prior to thrombolysis, each clot was perfused for 15 min to remove any debris weakly attached to its surface. Then, the suspension of the RGDS-modified microbubble was infused into the channel at a controlled flow rate to simulate a wall shear rate of 500 s^{-1} for 1 min, followed by infusion with degassed tPA (dissolved in saline) solution at the same flow rate while ultrasound was turned on for 5 min. The above steps were performed as a cycle. To ensure that the RGDS-modified microbubble adheres to the thrombus, we did not continuously expose the thrombus to ultrasound. Instead, manually turned the ultrasound output "on" for 5 min and "off" for 1 min. The suspension of the RGDS-modified microbubble was infused into the channel during ultrasound closure, allowing microbubble adhere to the thrombus. The entire sonothrombolysis procedure was performed for a total of 30 min. To maintain a shear rate of 500 s^{-1}, the degassed tPA solution was perfused into the channel at a controlled constant volumetric flow rate of 0.625 mL min^{-1} and a flow speed of 4.17 cm/s, whereas flow speeds ranging from 0 to 50 cm/s have been clinically documented in ischemic middle cerebral arteries [18]. The controlled constant flow rate was controlled by microinjection pumps. The calculation of the flow rate is shown in *Supplementary Material A*.

The microfluidic chip is a transparent straight polydimethylsiloxane (PDMS) channel. For the purpose of real-time observation of the sonothrombolysis process, a 1 MHz circular ultrasonic transducer (25-mm aperture diameter and 12.6-mm thickness, HNB-4P1-4225, Hainertec, Suzhou, China) made of the lead zirconate titanate piezoelectric ceramics (PZT-4) was positioned at a distance of 10 mm from the channel (Fig. 1B(ii)) for sonothrombolysis. The transducer was driven by an ultrasonic generator and operated in a continuous wave mode with variable intensity outputs. The frequency of the continuous wave ultrasound was 1 MHz, which is commonly used for sonothrombolysis [19]. The acoustic beam profile of the transducer was characterized using a hydrophone (NCS-1, Institute of Acoustics, Chinese Academy of Sciences) in a 23 cm × 15 cm × 23 cm tank, which frequency ranges from 200 kHz

to 6 MHz and effective tip size is 2 mm (*Supplementary Materials B*, Fig. S1). The acoustic pressure profile of the ultrasound transducer extends 40 mm laterally and 17 mm axially. The clot was located completely in the sound field. To generate acoustic waves and activate the microfluidic device, the ultrasound transducer was adhered to the PDMS microfluidic chip on a glass substrate using Ultrasound Gel (MIBO Technology Co., Guangdong, China) [19, 20]. Pressure amplitude in PDMS channel is shown in *Supplementary Material A* and *Supplementary Materials B*, Fig. S2.

In our experiments, we examined the effects of three ultrasound powers (1.5 W, 3 W, 6 W) on thrombus debris. The average acoustic pressure distribution in the channel region with a length of 20 mm was 1 MPa (1.5 W), 1.4 MPa (3 W), and 2 MPa (6 W), respectively.

After sonothrombolysis, the solution was centrifuged at 1500 rpm for 5 min at room temperature to destroy the residual microbubbles in the solution. After centrifugation, the supernatant was removed and the thrombus debris were resuspended with saline. The size and composition of the thrombus debris in the suspension were examined by the image particle size analyzer and confocal microscope.

Thrombus preparation

In the orthogonal test, the thrombus was prepared as follows: the whole-blood was obtained from the cubital veins of healthy volunteers who did not exhibit any signs of acute illness or coagulation disorders. In a blood collection tube containing 0.29 mol/L of Na-citrate (Vacuntainer, Becton-Dickinson, Germany), blood was drawn under standard conditions. Informed consent was obtained from all donors and all experiments were carried out in accordance with relevant laws and procedures approved by the Institutional Review Board (IRB) of Tsinghua University (Approval No. 18-CHS1). 50 μL saline containing 75 mM $CaCl_2$ and 35 mM $MgCl_2$ was added to 500 μL of whole blood to neutralize the anticoagulation effect of Na-citrate. Blood clots were incubated at 37 °C for 1 h.

All arterial thrombi were from four patients (one male and three females), aged from 45 to 78 years old. Informed consent was obtained from all donors. The patients were diagnosed with femoral or superior mesenteric artery embolism or stenosis. The thrombi were obtained by thrombectomy and were 4–6 mm in diameter and greater than 3 cm in length. Acute arterial thrombi were thrombosis within 7 days, while chronic thrombi were thrombosis greater than 1 month. The age of thrombus was determined based on the time between the onset of symptoms and the thrombectomy procedure in patients [21]. The experiment was approved by the Institutional Review Board (IRB) of Tsinghua University.

Thrombus histology

Histological evaluations of acute and chronic arterial thrombus were performed. Tissue samples were fixed with 10% formalin solution after being washed with 0.9% saline solution. Sections of tissues (5 μm) were obtained and processed. Tissues were stained with Martius Scarlet Blue (MSB) staining and Hematoxylin and Eosin (H&E) staining. Each tissue sample was analyzed using a light microscope (Olympus, Japan), and photomicrographs at a magnification of 20× were taken.

Thrombus sections were immunohistochemically examined for platelets (CD41). Heat-induced antigen retrieval was performed at 95 °C for 20 min using 0.3% sodium citrate (pH 6). Thrombus sections were washed in Tris-buffered saline (TBS) before staining, after which sections were blocked with 10% normal serum and 0.3% Triton-X 100 in TBS for 1 h. Next, sections were incubated with the primary antibody (Anti-CD41 antibody (ab63983, Abcam)) overnight at 4 °C. After washing 3 times for 5 min in TBS, the sections were blocked endogenous peroxidase activity for 15 min at RT with 0.3% hydrogen peroxide in TBS. Next, the sections were incubated in 1% BSA and TBS solution containing a biotinylated secondary anti-rabbit IgG antibody for 30 min at RT, followed by washing 3 times for 5 min in TBS. Then an appropriate amount of freshly prepared DAB or AEC solution was added and incubated for 5–8 min at RT. Finally, the nuclei were stained with hematoxylin and the results were examined under light microscopy.

Microbubble preparation

RGDS-modified microbubbles were prepared by adding 125 μL of 10 mg/mL RGDS (Batch No. 04010013130, Jiangsu Qiangyao Biological Technology Co. Ltd. Jiangsu, China) to every 5 mL of microbubbles (SonoVue, Bracco Suisse SA). The solution containing microbubbles and RGDS was then mixed in a mixer (DLAB, MX-RD-E) at 80 rpm for 10 min. Next, the solution was placed in a centrifuge (Eppendorf MiniSpin) and spun for 2 min at 800 rpm. Discarded the subnatant and added saline (0.9% NaCl) to the microbubble to the desired concentration. The microbubbles should be used immediately within 6 h of preparation.

Thrombus debris detection method

By measuring the particle size of the thrombus debris in the suspension after the sonothrombolysis, the relationship between the ultrasound power and thrombus debris is determined. Particle imaging and size analysis were performed on the solutions using an automatic image technique particle size analyzer (W-2000, Beijing Hangxin Tong

Technology Co.). To observe the structural composition of thrombus debris, we performed immunofluorescence staining of thrombus debris in the suspension. The thrombus debris in the suspension were fixed in 4% paraformaldehyde for 2 h on an adhesive glass slide. We blocked the slides for 1 h at RT with goat serum containing 0.3% Triton-X 100, and then treated them with primary antibodies overnight at 4 °C. The slides were then washed three times in PBS and then incubated with fluorescence-labeled secondary antibodies for 1 h at RT in the dark. After washing three times in PBS, slices were counterstained with Fluorescent mounting medium (ZLI-9556; ZSGB-Bio). The primary antibodies were as follows: Anti-CD41 antibody (ab63983, Abcam) and Anti-Fibrinogen beta chain (ab219355, Abcam). The secondary antibodies were conjugated to donkey anti-goat Alexa Fluor 488 (1:400; ab150129, Abcam) and goat anti-rabbit Alexa Fluor 647 (1:400; ab150079, Abcam). RBCs autofluorescence can be detected at 555 nm. Fluorescence was observed under a Laser Confocal Microscope Zeiss LSM780.

Data analysis

All experimental data are expressed as mean values ± SD. Students' t-tests and one-way analyses of variance (ANOVA) were used in each experiment for inter- and intragroup comparisons using the SPSS 19.0 software. Probability (P) values of < 0.05 are considered statistically significant.

Results

Orthogonal experiment

To study the effects of various factors on the size of thrombus debris during the sonothrombolysis process, three factors including ultrasound power, thrombolytic agents and microbubble concentration were selected as variable. The results are shown in *Supplementary Materials B* (Fig. S3). These data imply that the ultrasound power is the most important parameter, which has a significant effect on thrombus debris size, followed by thrombolytic agent concentration and microbubble concentration. Accordingly, subsequent investigation focused on the effects of ultrasound power on the size of thrombus debris, while those of the thrombolytic agent concentration and microbubble concentration were not further investigated.

Arterial thrombus

We performed an *in-vitro* thrombolysis study using arterial thrombi of different ages, which were taken from the abdominal aorta of different patients using surgical thrombectomy, as shown in Fig. 2. The age of the thrombus is determined based on the time between the onset of symptoms and the mechanical embolization procedure in the patient. Acute and chronic thrombi were placed into the homemade chambers for sonothrombolysis.

Acute thrombus forms within 7 days, while chronic thrombus lasts more than 1 months and is resistant to tPA [21, 22]. We characterized the components of acute and chronic arterial thrombi taken from patients by using tissue staining and scanning electron microscopy. The content of fibrin, red blood cells (RBCs) and platelets in the thrombi are shown in Fig. 2. In the sonothrombolysis, the thrombolytic drug lyses fibrin and the RGDS-modified microbubble targets to platelets, so this study focuses on the percentage of fibrin, platelets and RBCs in the thrombus. Acute thrombus has a wide range of components, with fibrin and RBCs as the major components ($40 \pm 6\%$, v/v and $43 \pm 5\%$, v/v, respectively), as shown in Fig. 2A-C. Whereas in chronic thrombus shown in Fig. 2D-F, fibrin is the main component of the thrombus ($66 \pm 3\%$). The proportion of RBCs in the thrombus is significantly lower ($17 \pm 2\%$), and the fraction of platelets varies less with the age of the thrombus. With aging, the density and size of fibrin fibers increased correspondingly (as shown in Fig. 2I, $P < 0.01$), which can be seen in SEM images of acute thrombus and chronic thrombus (Fig. 2G-H). As shown in Fig. 2I, the RBCs content was also significantly lower in chronic thrombus compared to that of acute thrombus ($P < 0.01$). The above results indicate that there is significant structural remodeling of the chronic thrombus after 7 days.
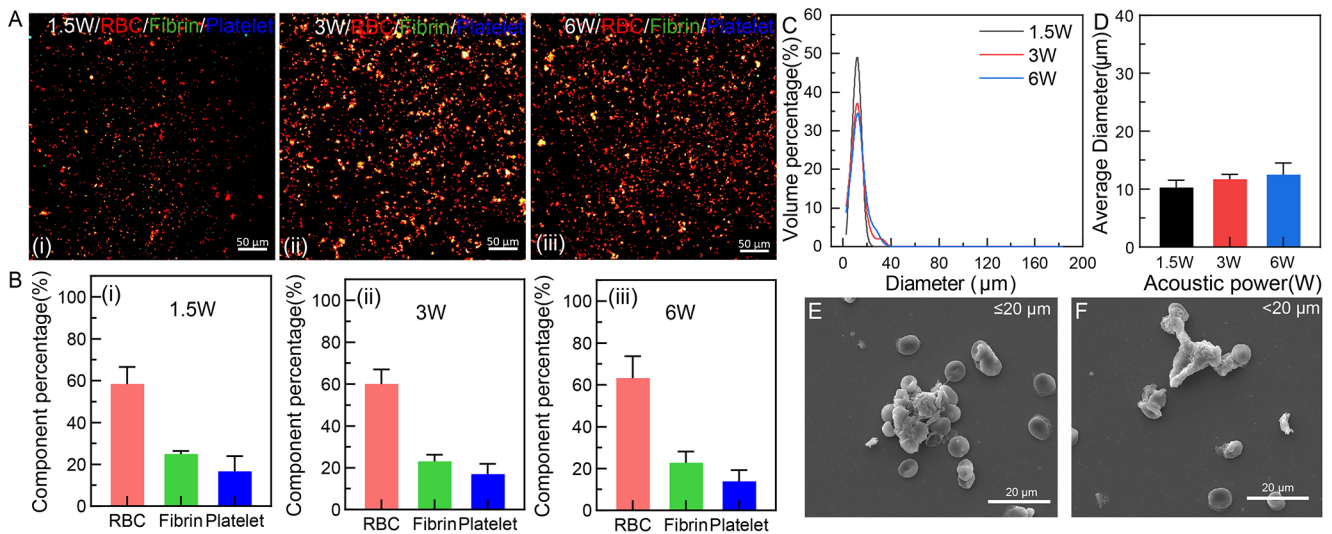
Effect of ultrasonic energy

To characterize the thrombus debris produced at different ultrasound powers, we performed the size and fraction analysis of thrombus debris from acute and chronic arterial thrombi after sonothrombolysis (Figs. 3 and 4). Sonothrombolysis in each group was performed for 30 min, using the same concentration of thrombolytic drug and microbubble. The ultrasound power were 1.5 W, 3 W and 6 W respectively. We conducted passive cavitation detection of the three ultrasound powers. As the ultrasound power increased, the inertial cavitation level gradually enhanced, as shown in *Supplementary Materials B* (Fig. S4). Other parameters of the ultrasound are shown in *Methods and Materials*. During sonothrombolysis, acute arterial thrombus dissolves faster than chronic arterial thrombus, and the characteristics of the resulting thrombus debris are also different. We fluorescently labeled fibrin (labeled green) and platelets (labeled blue) in the suspension by immunofluorescence technique, and RBCs can be detected as autofluorescence at 555 nm

Fig. 2 Characterization of acute and chronic arterial thrombi. The thrombus sections are stained with Hematoxylin & Eosin (H&E) staining, Martius Scarlet Blue (MSB) staining and an anti-platelet CD41 antibody. Classical H&E staining is used to visualize the composition and organization of overall acute thrombus (**A**) and chronic thrombus (**D**), and RBC-rich areas appear red whereas RBC-poor areas appear light pink. On MSB staining of acute thrombus (**B**) and chronic thrombus (**E**), red areas show the presence of fibrin, whereas RBC appear yellow. Platelets of acute thrombus (**C**) and chronic thrombus (**F**) are stained brown using an anti-CD41 antibody. Scale bar: 500 μm. The SEM images of acute thrombus (**G**) and chronic thrombus (**H**). Scale bar: 10 μm. (**I**) The component of acute thrombus and chronic thrombus in artery ($n = 6$, **: statistically different from acute thrombus, $P < 0.01$)
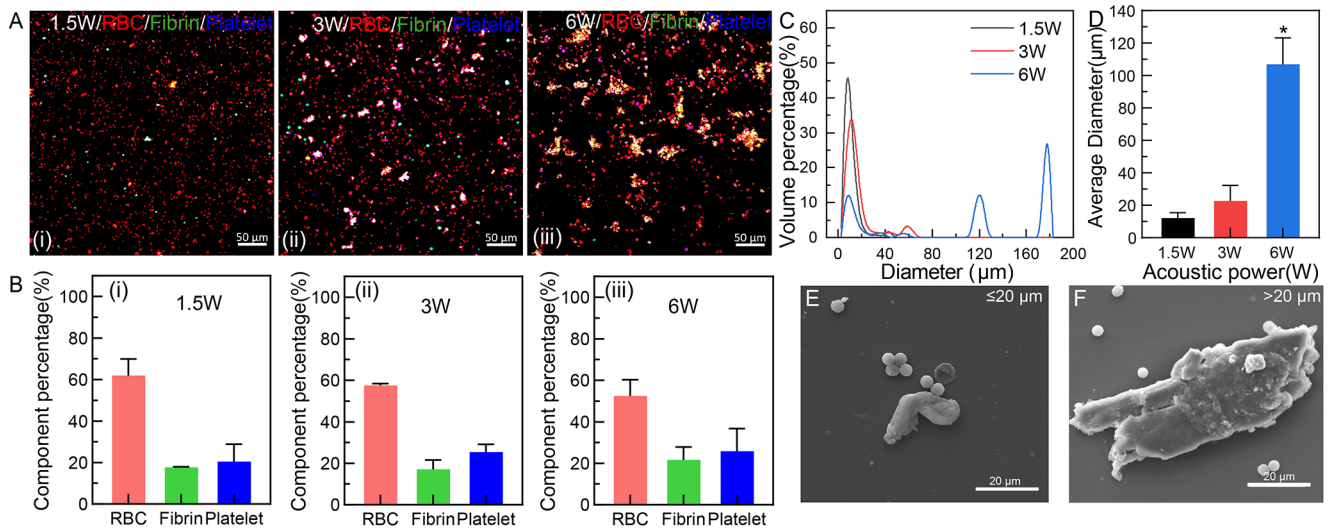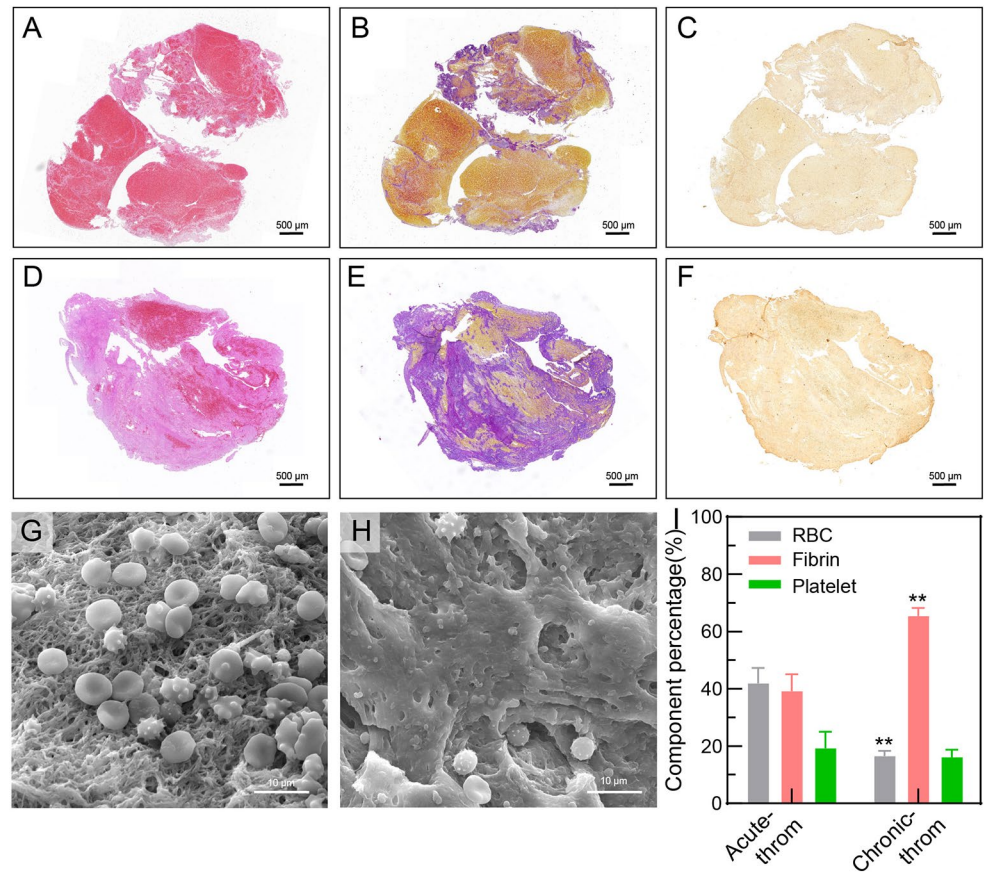
Fig. 3 The characteristics of acute arterial thrombus debris produced by different ultrasonic energy. (**A**) The merged fluorescent image of platelet, RBCs and fibrin. (i)-(iii) The ultrasonic energy is 1.5 W, 3 W and 6 W. The fibrin, platelets and RBCs in the thrombus debris under the fluorescence microscope are marked in green, blue and red, respectively. Scale bar: 50 μm. (**B**) Statistics of RBCs, fibrin and platelet content in thrombus debris. (i)-(iii) The ultrasonic energy is 1.5 W, 3 W and 6 W ($n = 3$). (**C**) Volume percentage of thrombus debris particles changes with ultrasound power. (**D**) In sonothrombolysis, the average diameter of thrombus debris particles varies with ultrasound power. (* $P < 0.05$) (**E**) and (**F**) The SEM images of the characteristic diameter of thrombus debris produced by sonothrombolysis of the acute arterial thrombus. Scale bar: 20 μm

Fig. 4 The characteristics of chronic arterial thrombus debris produced by different ultrasonic energy. (**A**) The merged fluorescent image of platelet, RBCs and fibrin. (i)-(iii) The ultrasonic energy is 1.5 W, 3 W and 6 W. The fibrin, platelets and RBCs in the thrombus debris under the fluorescence microscope are marked in green, blue and red, respectively. Scale bar: 50 μm. (**B**) Statistics of RBC, fibrin and platelet content in thrombus debris. (i)-(iii) The ultrasonic energy is 1.5 W, 3 W and 6 W ($n = 3$). (**C**) Volume percentage of thrombus debris particles changes with ultrasound power. (**D**) In sonothrombolysis, the average diameter of thrombus debris particles varies with ultrasound power. (* $P < 0.05$) (**E**) and (**F**) The SEM images of the characteristic diameter of thrombus debris produced by sonothrombolysis of the chronic arterial thrombus. Scale bar: 20 μm

(shown as red). We observed under confocal microscopy, as shown in Fig. 3A-B, and found that the components of thrombus debris produced has the highest RBCs content, followed by fibrin and platelets. However, there are little differences in the percentage of components of thrombus debris produced at different powers. In the group without ultrasound (only tPA), the size of the thrombus debris is small and uniform, and the dissolved thrombi are also less, as shown in *Supplementary Materials B* (Fig. S5). When the ultrasound power is 1.5 W, the debris are mainly composed of a single form of RBCs, platelets and fibrin, and a small amount of small-sized composite components consisting of small fragments of fibrin adhering to platelets or subcellular fragments, as shown in Fig. 3A(i). When the ultrasound power is 3 W, the thrombus debris exist in the form of RBCs and complexes. Among them, the larger size complex consists of RBCs, fibrin and platelets, and the smaller size complex consists of non-single components, as shown in Fig. 3A(ii). When the ultrasound power is 6 W, thrombus debris are also present in the form of RBCs and complexes. Among them, the complexes are mainly large-sized and compose of RBCs, fibrin and platelets, as shown in Fig. 3A(iii).

Our analysis of the size of thrombus debris shows that the size distribution of the thrombus debris generated in acute thrombus sonothrombolysis is not homogeneous. As shown in Fig. 3C, the peak plot of volume percentages of thrombus debris spans a wide range, with a maximum value of approximately 200 μm. Further, as shown in Fig. 3D, the

average diameter of thrombus debris increases significantly ($P < 0.05$) as the ultrasound power increases from 1.5 W to 6 W. The SEM pictures of acute thrombus debris similarly show that the smaller size debris, which are less than 20 μm in diameter, mostly consist of single component, while the larger size thrombus debris, which are larger than 20 μm in diameter, consist of platelets, RBCs and fibrin, as shown in Fig. 3E-F.

We also analyzed the thrombus debris produced by sonothrombolysis of chronic arterial thrombus (Fig. 4). They consist of more RBCs and small amounts of fibrin and platelets, as shown in Fig. 4A-C. In group without ultrasound (only tPA), the size of the thrombus debris is small and uniform, and there are fewer thrombi in dissolved. Thrombus debris are less than acute thrombus debris under the same conditions, as shown in *Supplementary Materials B* (Fig. S5). When the ultrasound power is 1.5 W, similar to acute thrombus debris, the thrombus debris consists mainly of single fractions of RBCs, platelets and fibrin, and a small amount of the complex consists of small fragments of fibrin adhering to platelets or subcellular fragments, as shown in Fig. 4A(i). When the ultrasound power are 3 W and 6 W, the thrombus debris consist of RBCs and small-sized complexes, respectively. Among them, the smaller size complex consists of any two or three components, as shown in Fig. 4A(ii)(iii). Similar to that of the sonothrombolysis of acute thrombus, the size of thrombus debris is smaller at the ultrasound power of 1.5 W. When the ultrasound power increases from 3 W to 6 W, the change of the size

and the average diameter of the thrombus debris particles are not significant, with a maximum thrombus debris size of approximately 30 μm, as shown in Fig. 4C-D. It indicates that ultrasonic energy has less effect on debris size of chronic thrombi during sonothrombolysis. Therefore, the chronic thrombus debris are small in size, and their composition are dominated by a simple structure, as shown in Fig. 4E-F.

Mechanism

To reveal the different sizes of thrombus debris generated under different ultrasound energies, we used a microfluidic chip for sonothrombolysis and observed the characteristics of thrombus debris shedding from the different ages of thrombi under ultrasound and microbubbles in real time. At the low ultrasound power, the cavitation produced by sonothrombolysis is not enough to disrupt the bond between fibrins. The debris being removed at this time range from single-cell debris to debris consisting of several interconnected blood cells, as shown in Fig. 5A(i) and Fig. 5B(i). The debris are similar to the size of the thrombus debris in group without ultrasound (only tPA), which are small and uniform, as shown in *Supplementary Materials B* (Fig. S5). However, in the sonothrombolysis of acute thrombi, high ultrasound power causes the thrombus to break from the inside, resulting in large-sized thrombus debris that are large clusters of thousands of blood cells. These blood cells are still connected to each other by partially dissolved fibrin fibers. It also can be clearly seen from the colors of the debris, as shown in Fig. 5A(ii)-(iii) and *Supplementary Materials C* (Video S1). The presence of this debris increases the possibility of further embolism in the microvasculature downstream of the thrombus site [23]. However, in the observation of sonothrombolysis of chronic thrombi, we did not find an increase in the size of debris with the increasing of ultrasound power (Fig. 5B(ii)-(iii)). The analysis of the size of thrombus debris shows that acute thrombus is more sensitive to ultrasonic energy. This may be due to the differences in the density and size of fibrin within acute and chronic thrombi (Fig. 2G-H). Therefore, the mechanical effect of cavitation in acute thrombus tears more and larger thrombus debris off the thrombus. However, the threshold of thrombus resistance to tearing becomes higher in chronic thrombus, and the mechanical tearing force generated by cavitation is not enough to remove larger thrombus debris from the thrombus.
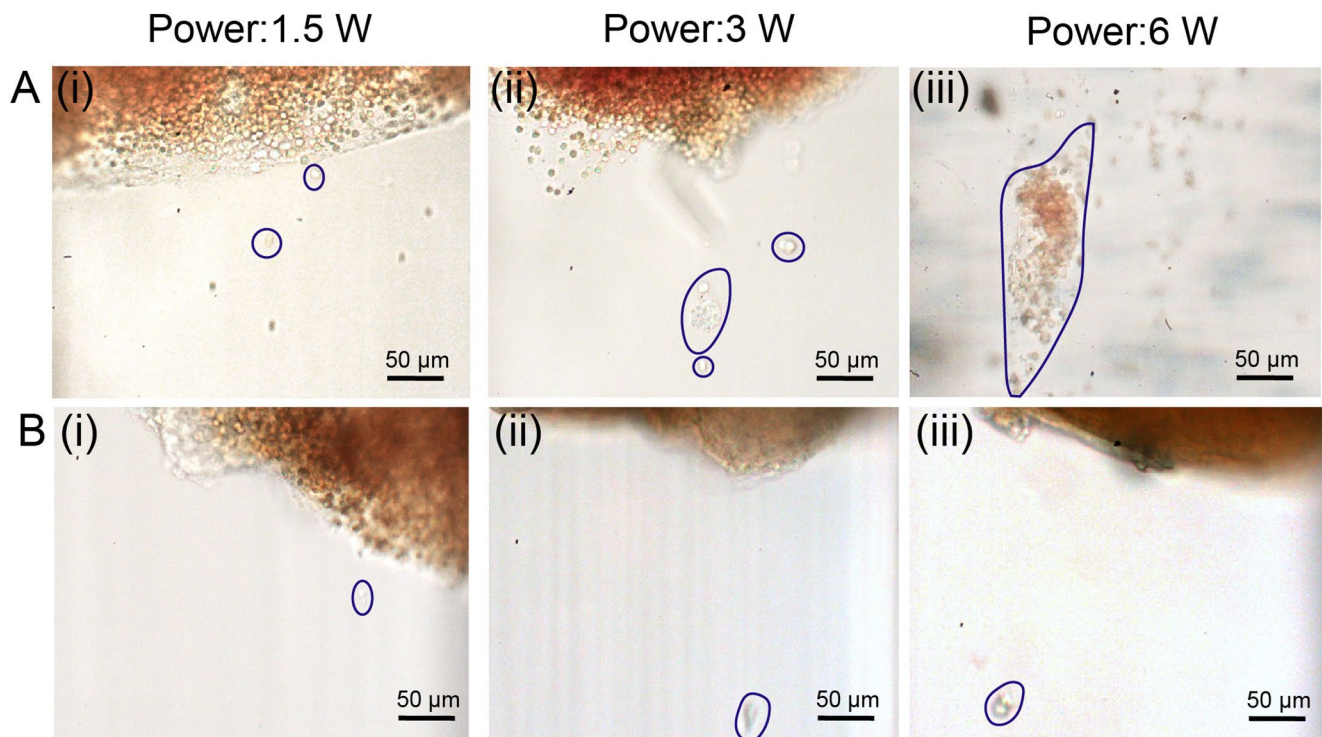
Fig. 5 Real-time observation of the shedding of thrombus debris. (A) Three representative optical microscopy images of removed larger thrombus debris (encircled) in acute arterial sonothrombolysis with (i) low (1.5 W), (ii) medium (3 W), and (iii) high ultrasound power (6 W). (B) Three representative optical microscopy images of removed larger thrombus debris (encircled) in chronic arterial sonothrombolysis with (i) low (1.5 W), (ii) medium (3 W), and (iii) high ultrasound power (6 W). Scale bar: 50 μm

Discussion

Microbubble-assisted sonothrombolysis has great potential in the treatment of vascular thromboembolic diseases. However, large thrombus debris, which may form after thrombolysis, can increase the danger of obstructing downstream vessels and, in the most severe case, lead to stroke or pulmonary embolism [8]. This study focused on exploring the effect of ultrasound energy on thrombus debris. The acute and chronic thrombi used in this article are different in the structures. The differences of their structures may make them show different sensitivities to sonothrombolysis [22]. By comparing the composition and size of thrombus debris particles and observing the shedding characteristic of thrombus debris in real time, our study presents the characteristics of debris particles generated under different ultrasound energies on various kinds of thrombus during sonothrombolysis. In our results, acute thrombus is an early stage of thrombus with a looser structure and insufficient crosslinking between fibrin. However, fibrin contracts under the traction of platelets over time, the fibrotic connective tissue component of the thrombus increases and the thrombus structure becomes more denser and firmer when chronic thrombus is more than 7 days old [21]. In the previous studies, thrombolysis is a biochemical and mechanical process in which mechanical forces work in combination with biochemical fibrinolytic processes to achieve effective thrombolysis, however each process works inefficiently when acting on its own [24]. Particularly, in a non-occlusive thrombosis model where a dense thrombus adheres to the vessel wall, the dense thrombus is less sensitive to thrombolysis in the absence of flow mechanical force, and the drug does not penetrate easily into the thrombus [25].

The mechanisms involved in microbubble-mediated sonothrombolysis to induce thrombus rupture are acoustic cavitation and pharmacological thrombolysis. Acoustic cavitation is the dynamical response of a bubble driven by acoustic stress in liquids or other media. Cavitation is usually classified into two categories: stable cavitation and inertial cavitation [26]. Acoustic cavitation usually forms microfluidic or high-velocity microjets near the thrombus, and the ensuing shear stress acts on the thrombus and accelerates the diffusion of thrombolytic drug particles into the fibrin [27, 28]. The severe shear stress can also alter RBC membranes [9], break fibrin bonds, affect platelets, and lead to thrombus breakdown [29]. In our experiments, when the ultrasonic energy rises, the acoustic pressure increases, the cavitation activity enhanced, and the mechanical force acting on the thrombus rises as well. In the study by Maxwell et al., high pressures produced more large-sized thrombus debris particles than low pressures [9]. Similar results were observed in our work in acute arterial thrombus with sonothrombolysis, but not in chronic arterial thrombus.

In a mathematical model studying the molecular dynamics of thrombolysis [30], blood clots are assumed to be mechanically stable assemblies of blood cells that are interconnected with fibrin bonds, which are exposed to biochemical degradation of thrombolytic agents and the mechanical forces of blood flow. However, in this study, the flow rates were consistent among the groups and therefore did not affect the experimental comparison results. In microbubble-mediated sonothrombolysis, both the chemical action of thrombolytic agents and the mechanical forces generated by ultrasound act on the fibrin network, causing it to depolymerize under chemical and mechanical action. The use of a thrombolytic drug can greatly reduce the level of mechanical force required for clot disintegration [30]. The main component of arterial thrombus is fibrin [31], and there are certain interactions between fibrin and fibrin, fibrin and platelets. Therefore, during the sonothrombolysis of acute thrombus in our study, thrombolytic agent is more easily to penetrate the thrombus, lowering the mechanical force needed for breakdown. The mechanical force generated by ultrasound can just match the level of mechanical force required for thrombus breakdown, making it easier to rupture and tearing apart many of the large-sized thrombus debris. However, in the sonothrombolysis of chronic thrombus in our experiment, the thrombolytic agent does not easily enter the interior of the thrombus, and the mechanical effect of ultrasound cannot reach the level of mechanical force required for the rupture between fibrins. At this point, no matter how the ultrasound energy changes, the size of the debris is not affected. It can be concluded that in ultrasound-assisted enhanced thrombolysis, ultrasound energy has a greater effect on the size of the acute thrombus debris.

In this work, we explored the effect of ultrasound energy on debris particles during sonothrombolysis of different types of thrombi in a microfluidic channel. Although unlike laminar flow in microchannels, turbulent flow is likely to occur in larger vessels. The mechanical forces of streaming blood on the thrombus surface are much higher in turbulent flow than in laminar flow, which may promote thrombolysis [24]. Nevertheless, there are also stable and laminar flow conditions in the circulatory system [32].

Another question is that this work uses microchannel with continuous wave ultrasound, which may result in a heterogenous standing wave fields. We will adapt and improve the experimental setup to approach the real sonothrombolysis process in the true vascular in the future studies.

Conclusions

In this study, we investigate the degree of influence of ultrasound power, thrombolytic agent and microbubble concentration on thrombus debris in sonothrombolysis using an orthogonal test design. The results show that ultrasound energy have a greater effect on thrombus debris. Further, we explore the effect of ultrasound power on different ages of arterial thrombus debris during sonothrombolysis. The results show that in acute arterial thrombus, the size of debris produced during sonothrombolysis is related to the ultrasound power. In contrast, in the sonothrombolysis of chronic thrombus, ultrasound power has less effect on the size of thrombus debris. To explain the mechanism by which ultrasound energy affects the size and fraction of thrombus debris during sonothrombolysis of different ages thrombus, we performed sonothrombolysis using microfluidic chips and observed the morphology and detachment process of thrombus debris in real time. It is found that the mechanical action of ultrasound and the biochemical action of thrombolytic drugs work synergistically during sonothrombolysis. The structure of the thrombus varies at different ages, as does the binding between the components within the thrombus. The different forces that need to be resisted by the biochemical action of the thrombolytic drugs and the mechanical action of ultrasound lead to different rupture degrees of the thrombus, resulting in different components and sizes of debris. This study may help to better utilize the parameters of sonothrombolysis to achieve lysis of arterial thrombi at different ages and may also help to implement safer thrombolysis strategies in the clinical.

Declarations

References

1. Tsao CW, Aday AW, Almarzooq ZI et al (2023) Heart disease and stroke statistics—2023 update: a report from the American Heart Association. Circulation 147:e93–e621
2. Donnan GA, Davis SM, Parsons MW et al (2011) How to make better use of thrombolytic therapy in acute ischemic stroke. Nat Reviews Neurol 7:400–409
3. Goncalves A, Su EJ, Muthusamy A et al (2022) Thrombolytic tPA-induced hemorrhagic transformation of ischemic stroke is mediated by PKCβ phosphorylation of occludin. Blood J Am Soc Hematol 140:388–400
4. Meairs S, Alonso A, Hennerici MG (2012) Basic science advances for clinicians. Stroke 43:1706–1710
5. Alexandrov AV, Molina CA, Grotta JC et al (2004) Ultrasound-enhanced systemic thrombolysis for acute ischemic stroke. N Engl J Med 351:2170–2178
6. Suo D, Govind B, Gu J et al (2019) Dynamic assessment of dual-frequency microbubble-mediated sonothrombolysis in vitro. J Appl Phys 125(8)
7. Goel L, Jiang X (2020) Advances in sonothrombolysis techniques using piezoelectric transducers. Sensors 20(5):1288
8. Chueh JY, Kühn AL, Puri AS et al (2013) Reduction in distal emboli with proximal flow control during mechanical thrombectomy: a quantitative in vitro study. Stroke 44:1396–1401
9. Maxwell AD, Cain CA, Duryea AP et al (2009) Noninvasive thrombolysis using pulsed ultrasound cavitation therapy–histotripsy. Ultrasound Med Biol 35:1982–1994
10. Rosenschein U, Furman V, Kerner E et al (2000) Ultrasound imaging–guided noninvasive ultrasound thrombolysis: preclinical results. Circulation 102:238–245
11. Bader KB, Bouchoux G, Holland CK (2016) Sonothrombolysis Therapeutic Ultrasound 339–362
12. Xu S, Zong Y, Feng Y et al (2015) Dependence of pulsed focused ultrasound induced thrombolysis on duty cycle and cavitation bubble size distribution. Ultrason Sonochem 22:160–166
13. Laccourreye O, Laurent A, Polivka M et al (1993) Biodegradable starch microspheres for cerebral arterial embolization. Invest Radiol 28:150–154
14. Goel L, Wu H, Zhang B et al (2021) Nanodroplet-mediated catheter-directed sonothrombolysis of retracted blood clots. Microsystems Nanoengineering 7:3
15. Kim J, Bautista KJB, Deruiter RM et al (2021) An analysis of sonothrombolysis and cavitation for retracted and unretracted clots using microbubbles versus low-boiling-point nanodroplets. IEEE Trans Ultrason Ferroelectr Freq Control 69:711–719
16. Papadopoulos N, Kyriacou PA, Damianou C (2017) Review of protocols used in ultrasound thrombolysis. J Stroke Cerebrovasc Dis 26:2447–2469
17. Nedelmann M, Eicke BM, Lierke EG et al (2002) Low-frequency ultrasound induces nonenzymatic thrombolysis in vitro. J Ultrasound Med 21:649–656
18. Alexandrov AV, Tsivgoulis G, Rubiera M et al (2010) End-diastolic velocity increase predicts recanalization and neurological improvement in patients with ischemic stroke with proximal arterial occlusions receiving reperfusion therapies. Stroke 41:948–952

19. Gao Y, Wu M, Gaynes BI et al (2021) Study of ultrasound thrombolysis using acoustic bubbles in a microfluidic device. Lab Chip 21:3707–3714

20. Salari A, Appak-Baskoy S, Coe IR et al (2021) Dosage-controlled intracellular delivery mediated by acoustofluidics for lab on a chip applications. Lab Chip 21:1788–1797

21. Hendley SA, Dimov A, Bhargava A et al (2021) Assessment of histological characteristics, imaging markers, and rt-PA susceptibility of ex vivo venous thrombi. Sci Rep 11:22805

22. Czaplicki C, Albadawi H, Partovi S et al (2017) Can thrombus age guide thrombolytic therapy. Cardiovasc Diagnosis Therapy 7:S186

23. Herrera S, Comerota AJ (2011) Embolization during treatment of deep venous thrombosis: incidence, importance, and prevention. Tech Vasc Interv Radiol 14:58–64

24. Bajd F, Vidmar J, Blinc A et al (2010) Microscopic clot fragment evidence of biochemo-mechanical degradation effects in thrombolysis. Thromb Res 126:137–143

25. Tratar G, Blinc A, Štrukelj M et al (2004) Turbulent axially directed flow of plasma containing rt-PA promotes thrombolysis of non-occlusive whole blood clots in vitro. Thromb Haemost 91:487–496

26. Stride E, Coussios C (2019) Nucleation, mapping and control of cavitation for drug delivery. Nat Reviews Phys 1:495–509

27. Collis J, Manasseh R, Liovic P et al (2010) Cavitation microstreaming and stress fields created by microbubbles. Ultrasonics 50:273–279

28. Crum LA (1988) Cavitation microjets as a contributory mechanism for renal calculi disintegration in ESWL. J Urol 140:1587–1590

29. Westermark S, Wiksell H, Elmqvist H et al (1999) Effect of externally applied focused acoustic energy on clot disruption in vitro. Clin Sci 97:67–71

30. Bajd F, Serša I (2013) Mathematical modeling of blood clot fragmentation during flow-mediated thrombolysis. Biophys J 104:1181–1190

31. Chernysh IN, Nagaswami C, Kosolapova S et al (2020) The distinctive structure and composition of arterial and venous thrombi and pulmonary emboli. Sci Rep 10:5112

32. van Hinsbergh V, Stein C, Brown N et al (2019) Disturbed laminar blood flow causes impaired fibrinolysis and endothelial fibrin deposition in vivo. Thromb Haemost 119:223–233

Authors and Affiliations

Xiaobing Zheng[1] · **Yunfan Pan[1]** · **Zhaojian Wang[2]** · **Shuguang Zhang[1]**

✉ Xiaobing Zheng
zxb19@mails.tsinghua.edu.cn

✉ Shuguang Zhang
shuguang0502@163.com

1   State Key Laboratory of Tribology, Department of Mechanical Engineering, Tsinghua University, Beijing 100084, China

2   Peking Union Medical College Hospital, Chinese Academy of Medical Sciences, Beijing 100730, China